Materials Science Forum Vols. 408-412 (2002) pp. 1645-1650
online at http://www.scientific.net

Computer Simulation of Martensitic Transformation in Constrained Films

D.J. Seol[1], S.Y. Hu[2], Y.L. Li[2], L.Q. Chen[2] and K.H. Oh[1]

[1] School of Materials Science and Engineering, Seoul National University, San 56-1, Shirim-dong, Gwanak-gu, Seoul 151-742, Korea

[2] Department of Materials Science and Engineering, The Pennsylvania State University, University Park, PA 16802, USA

Keywords: Cubic-to-Tetragonal, Martensitic Transformation, Phase-Field Model, Thin Films

Abstract. 3-dimensional phase-field model is developed to describe the cubic to tetragonal martensitic phase transformation in thin film attached to a substrate. Elastic solutions are derived for both elastically anisotropic and isotropic thin films with arbitrary domain structures, subject to the mixed stress-free and constraint boundary conditions. Nucleation process as well as final domain structure strongly depends on the substrate constraint. Lower undercooling results in less volume fraction of martensite, finer domain structure and longer nucleation period.

Introduction

Martensitic transformation (MT) takes place in many engineering materials. The properties of transforming materials are strongly affected by the generated martensitic phase in both bulk and thin film materials under constraint [1]. Interest in the martensitic transformation in constrained thin films has increased recently due to growing applications of ferroelectric, ferromagnetic materials and shape memory alloys. In the martensitic transformation, the crystal lattice mismatch between parent phase and martensitic phase produces the strain energy that is the most important factor responsible for all specific features of the martensitic transformation such as martensitic morphology, transformation hysteresis, thermoelastic equilibrium and shape memory effect [2].
Phase-field models provide a convenient basis for the numerical solution of complicated pattern evolution of transforming phases because all the governing equations are written as unified ones in the whole space of system. Phase-field model has been successfully applied to the prediction of martensitic microstructure evolution in bulk materials [1,2,3] and ferroelectric materials in thin film [4]. In this work, 3-dimensional phase-field model is developed to provide a realistic simulation of cubic to tetragonal martensitic transformation in thin film elastically constrained by a substrate. The effect of substrate constraint and undercooling on the final microstructure and transformation kinetics is studied.

Phase-field model of cubic to tetragonal martensitic transformation

The simulation of cubic to tetragonal MT with phase-field approach requires phase fields of three lro parameters, η_1, η_2, η_3. The temporal evolution of phase field is described by the time-dependent Ginzburg-Landau kinetic equation:

$$\frac{\partial \eta_i(\bar{r},t)}{\partial t} = -L_i \frac{\delta F}{\delta \eta_i(\bar{r},t)} + \xi_i(\bar{r},t) = -L_i\left(\frac{\partial f}{\partial \eta_i} - \beta_i \nabla^2 \eta_i + \mu_{el}\right) + \xi_i(\bar{r},t) \qquad (1)$$

where $\bar{r}$ is the position vector, F is total free energy of a system, L_i is the phase-field mobility, $\xi_p(\bar{r},t)$ is the thermal noise term, β_i is the gradient energy coefficient, and μ_{el} is a derivative of elastic energy density function with respect to lro parameters. The total free energy of a system consists of bulk chemical free energy, interface energy, elastic energy, free energy by

applied field and so on. The interface energy is related to $\beta_i \nabla^2 \eta_i$. The chemical free energy density, f, is approximated by Landau-type fourth-order polynomial consisting of the cubic symmetry invariants of the lro parameters [2],

$$f_0(\eta_1,\eta_2,\eta_3)^* = f_0(0,0,0)^* + \frac{1}{2}A_1^*(\eta_1^2+\eta_2^2+\eta_3^2) - \frac{1}{3}A_2^*(\eta_1^3+\eta_2^3+\eta_3^3) + \frac{1}{4}A_3^*(\eta_1^2+\eta_2^2+\eta_3^2)^2 \qquad (2)$$

where $f_0(\eta_1,\eta_2,\eta_3)^* = f_0(\eta_1,\eta_2,\eta_3)/|\Delta f|$, $|\Delta f|$ is the transformation driving force defined as $|\Delta f| = |f_0(\eta_0,0,0) - f_0(0,0,0)|$, which is the difference between the free energy minimum and the free energy of parent phase, η_0 is the equilibrium value of the lro parameter in the martensite phase, and A_1^*, A_2^*, A_3^* are the dimensionless parameters. Equation (2) provides a local minimum at $\eta_1 = \eta_2 = \eta_3 = 0$ corresponding to the metastable parent phase and global minima at $\eta_1 = \eta_0$, $\eta_2 = \eta_3 = 0$, $\eta_2 = \eta_0$, $\eta_1 = \eta_3 = 0$, $\eta_3 = \eta_0$, $\eta_1 = \eta_2 = 0$ corresponding to three orientation variants of the stable martensitic phases.

To describe the elastic energy caused by a local evolution of microstructure, the stress-free strain needs to be defined. The stress-free strain caused by the change of crystal lattice parameter from cubic to tetragonal lattice is characterized by,

$$\varepsilon_{ij}^0(\vec{r}) = \sum \varepsilon_{ij}^{\eta}(p)\left(\frac{\eta_p}{\eta_0}\right) = \frac{\eta_1(\vec{r})}{\eta_0}\begin{bmatrix}\varepsilon_3 & 0 & 0\\ 0 & \varepsilon_1 & 0\\ 0 & 0 & \varepsilon_1\end{bmatrix} + \frac{\eta_2(\vec{r})}{\eta_0}\begin{bmatrix}\varepsilon_1 & 0 & 0\\ 0 & \varepsilon_3 & 0\\ 0 & 0 & \varepsilon_1\end{bmatrix} + \frac{\eta_3(\vec{r})}{\eta_0}\begin{bmatrix}\varepsilon_1 & 0 & 0\\ 0 & \varepsilon_1 & 0\\ 0 & 0 & \varepsilon_3\end{bmatrix} \qquad (3)$$

where, $\varepsilon_1 = (a - a_c)/a_c$, $\varepsilon_3 = (c - a_c)/a_c$, a, c are the crystal lattice parameters of the tetragonal stress-free martensitic phase, and a_c is the crystal lattice parameter of the cubic parent phase.

In the linear elasticity, the stress σ_{ij} is related to the elastic strain by the Hooke's law:

$$\sigma_{ij} = c_{ijkl}\left(\varepsilon_{kl}(\vec{r}) - \varepsilon_{kl}^0(\vec{r})\right) \qquad (4)$$

where $\varepsilon_{kl}(\vec{r})$ is the total strain measured with respect to a reference lattice. The total strain can be separated into homogeneous and heterogeneous strains [5]:

$$\varepsilon_{ij}(\vec{r}) = \bar{\varepsilon}_{ij} + \delta\varepsilon_{ij}(\vec{r}) \qquad (5)$$

where the heterogeneous strain, $\delta\varepsilon_{ij}(\vec{r})$, is defined so that

$$\int_V \delta\varepsilon_{ij}(\vec{r})d^3r = 0 \qquad (6)$$

The homogeneous strain is the uniform macroscopic strain characterizing the macroscopic shape and volume change associated with the total strain. The strain and displacement relationship gives the following equation:

$$\delta\varepsilon_{ij}(\vec{r}) = \frac{1}{2}\left[\frac{\partial u_i(\vec{r})}{\partial r_j} + \frac{\partial u_j(\vec{r})}{\partial r_i}\right] \qquad (7)$$

where $u_i(\vec{r})$ denotes the ith component of displacement.
The mechanical equilibrium equations with respect to elastic displacements are expressed as

$$\frac{\partial \sigma_{ij}}{\partial r_j} = 0 \tag{8}$$

where r_j is the jth component of $\vec{r}$. The stress-free boundary condition at the top surface of a film is given by

$$\sigma_{i3}\big|_{x_3=h_f} = 0 \tag{9}$$

where h_f is the film thickness along z direction. Since the elastic perturbation resulted from the heterogeneous strain disappears in the substrate far from the film-substrate interface, the following condition is used to describe the constraint of the substrate

$$u_i\big|_{x_3=-h_s} = 0 \tag{10}$$

where h_s is the distance from the film-substrate interface into the substrate, beyond which the elastic deformation is ignored.

To solve Eqs. (8)-(10), two elastic solutions are superposed[4]. First solution is from Khachaturyan's microelasticity theory[5] within $0 < x_3 < h_f$ and second one is from the elastic solution in an infinite plate of thickness $h_f + h_s$, satisfying the two boundary conditions. Consequently, the elastic energy in the constrained thin film can be calculated from Eqs. (4), (5) and (7).

The dimensionless form of Eq. (1) becomes

$$\frac{\partial \eta_i(\vec{r}^*,t^*)}{\partial t^*} = -\left(\frac{\partial f^*}{\partial \eta_i} - \beta_i^* \nabla^{*2}\eta_i + \mu_{el}^*\right) + \xi_i^*(\vec{r}^*,t^*) \tag{11}$$

where $r^* = r/l_0$, $t^* = tL|\Delta f|$ and $\beta_i^* = \beta_i/((\Delta x)^2|\Delta f|)$, where l_0 is the grid spacing.
Taking a Foutier-transform of both sides of Eq. (11) gives

$$\frac{\partial \eta_i(\vec{g}^*,t^*)}{\partial t^*} = -\left(\left(\frac{\partial f^*}{\partial \eta_i}\right)_{\vec{g}^*} + \beta_i^*(g^*)^2\eta_i(\vec{g}^*,t^*) + \mu_{el}^*(\vec{g}^*)\right) + \xi_i^*(\vec{g}^*,t^*) \tag{12}$$

where g^* is the magnitude of $\vec{g}^*$, $\eta_i(\vec{g}^*,t^*)$, $\mu_{el}^*(\vec{g}^*)$ and $\xi_i^*(\vec{g}^*,t^*)$ are the Fourier transforms of $\eta_i(\vec{r}^*,t^*)$, $\mu_{el}^*(\vec{r}^*)$ and $\xi_i^*(\vec{r}^*,t^*)$, respectively. The above equation can be efficiently solved using a semi-implicit method [6],

$$\eta_i(\vec{g}^*,t^*+\Delta t^*) = \frac{\eta_i(\vec{g}^*,t^*) - \Delta t^*\left[\left(\frac{\partial f^*}{\partial \eta_i}\right)_{\vec{g}^*} + \mu_{el}^*(\vec{g}^*)\right]}{1+\beta_i(g^*)^2\Delta t^*} + \tilde{\xi}_i^*(\vec{g}^*,t^*) \tag{13}$$

where $\tilde{\xi}_i^*(\vec{g}^*,t^*) = \Delta t^* \xi_i^*(\vec{g}^*,t^*)/\left(1+\beta_i(g^*)^2\Delta t^*\right)$ and Δt^* is the time step for integration.

Simulation procedure

In the computer simulations, $128\times128\times32$ discrete grid points are used, and periodic boundary conditions are applied along x_1 and x_2 axes. The dimensionless grid spacing in real space is chosen to be $\Delta x_1/l_0 = \Delta x_2/l_0 = 1.0$ and $\Delta x_3/l_0 = 0.5$ and Δt^* is chosen to be 0.01. The transformation strains used in this study are those of Fe-31%Ni alloy with $\varepsilon_1 = 0.1322$ and $\varepsilon_3 = -0.1994$ [7]. The elastic constants of the Fe-31%Ni alloy are reported as $c_{11} = 1.404\times10^{11}$ Pa and $c_{12} = 0.84\times10^{11}$ Pa [8]. The dimensionless parameters A_1^*, A_2^* and A_3^* in the chemical free energy equation are chosen to be 0.1, 1.65 and 0.8, respectively. The gradient energy coefficient β_i^* is chosen to be 0.5. The Gaussian random noise is applied for the time period of $t^* = 2.0$ to simulate the nucleation of martensitic phase. To investigate the effect of undercooling on the martensitic microstructure evolution, a dimensionless ratio between elastic energy and chemical energy, ζ, is introduced [2].

$$\zeta = \frac{c_{ijkl}\varepsilon_{ij}^0\varepsilon_{kl}^0}{\Delta f} \tag{14}$$

Results and discussion

The effect of substrate constraint on microstructure has been investigated with the Fe-31%Ni material and $\zeta = 10$. Figure 1 shows the change of microstructure according to different mismatch strains between film and substrate. The microstructure and volume fraction of each domain are strongly dependent on the mismatch strain. When the mismatch strain is zero, the martensitic phase consists of 50% η_1 and 50% η_2 domains. The two domains in Fig. 1(a) are alternating $\{110\}$ twin-related orientation variants and form polytwinned plates. As the mismatch strain become more tensile, η_3 domain become more favorable and the volume fraction of η_3 domain increases up to 31% and 75% of total martensitic phase as shown in Fig. 1(b) and (c), respectively.

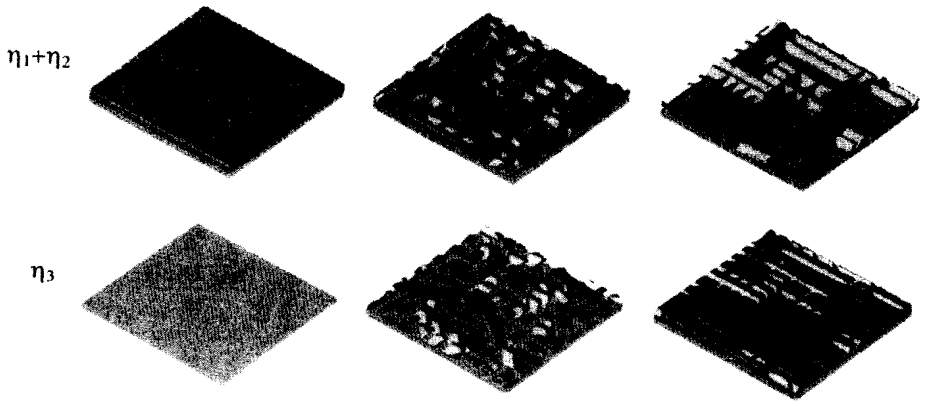

(a) $\bar{\varepsilon} = 0.0$ (b) $\bar{\varepsilon} = 0.02$ (c) $\bar{\varepsilon} = 0.05$

Fig. 1 Microstructures obtained at various substrate constraints with the transformation strain of the Fe-31%Ni material and $\zeta = 10$.

Figure 2 shows an initial microstructure evolution of martensitic transformation on top surface without mismatch strain. Dark and bright fields correspond to η_1 and η_2 domains, respectively. From the very early stage of nucleation, dark and bright fields coexist like a nucleation pair to accommodate strain energy. Since the elastic energy plays an important role in martensitic transformation, complex nuclei is more favorable in terms of strain accommodation. The single variant nucleus would create a long-range stress field with a large strain energy proportional to the nucleus volume [2].

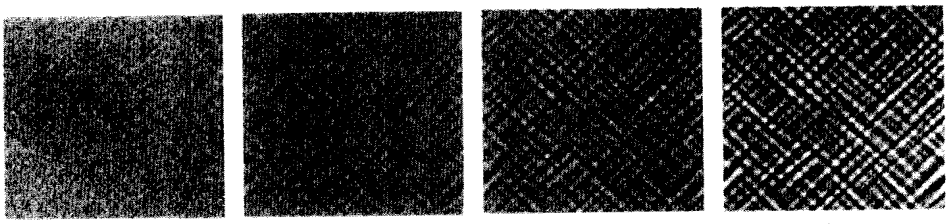

(a) $t^* = 1.0$ (b) $t^* = 2.0$ (c) $t^* = 2.5$ (d) $t^* = 3.0$

Fig. 2 Initial microstructure evolution of martensitic transformation on top surface without mismatch strain.

Figures 3 and 4 show the change of domain volume fractions versus time when $\bar{\varepsilon} = 0.0$ and $\bar{\varepsilon} = 0.04$, respectively. The kinetic curves with zero mismatch strain show the simultaneous development of η_1 and η_2 domains after a nucleation period (Fig. 3). When $\bar{\varepsilon} = 0.04$, the kinetic curves show that η_1 and η_2 domains develop after η_3 domain forms first (Fig. 4). In both cases, once the transformation starts after the nucleation, the transformation is completed in a short time period. The nucleation period become longer as ζ increases, because the increased ζ means lower undercooling and increased elastic energy compared to the chemical energy. Low undercooling ($\zeta = 15$) results in less volume fraction of martensitic phase, and finer microstructures due to the increased elastic energy effect.

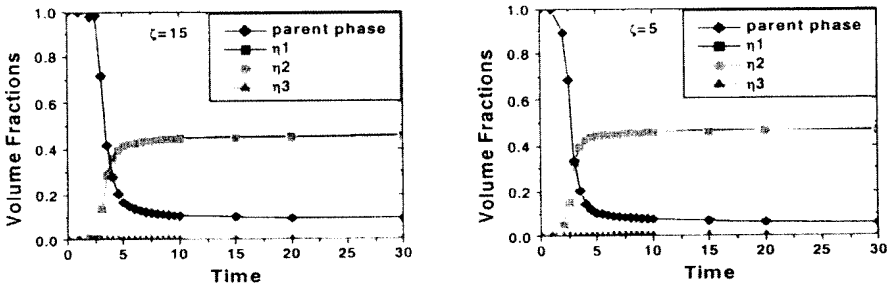

(a) $\zeta = 15$ (b) $\zeta = 5$

Fig. 3 Change of domain volume fractions versus time without mismatch strain

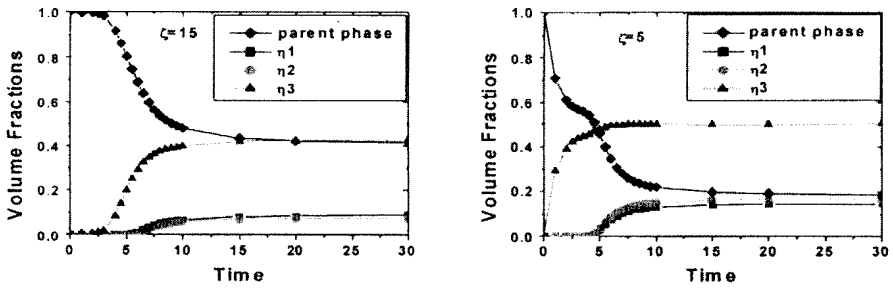

(a) $\zeta = 15$ (b) $\zeta = 5$

Fig. 4 Change of domain volume fractions versus time with $\bar{\varepsilon} = 0.04$

Conclusion

A 3-D phase-field model for the cubic to tetragonal martensitic transformation is developed to predict the evolution of martensitic microstructure in thin film elastically constrained by substrate. The microstructure strongly depends on the substraint constraint represented by mismatch strain. With the transformation strain of Fe-31%Ni material, the martensitic phase in the film consists of polytwinned plates formed by alternating $\{110\}$ twin-related η_1 and η_2 variants under zero mismatch strain, and the fraction of η_3 increases as the mismatch strain becomes tensile. Strain accommodation starts from the nucleation process by forming complex nuclei of η_1 and η_2 under zero mismatch strain. The increase in ζ, which means low undercooling, results in less martensitic volume fraction, finer domain morphology and longer nucleation period.

Acknowledgement. Authors are grateful for the financial support for this research by the National Research Laboratory Project through the Ministry of Science and Technology and by the US National Science Foundation under grant number DMR-01-22638.

References

[1] A.Artemev, Y.Wang and A.G.Khachaturyan: *Acta Mater.*, Vol. 48 (2000), p.2503.
[2] A.Artemev, Y.Jin and A.G.Khachaturyan: *Acta Mater.*, Vol. 49 (2001), p.1165.
[3] Y.M.Jin, A.Artemev and A.G.Khachaturyan: *Acta Mater.*, Vol. 49 (2001), p.2309.
[4] Y.L.Li, S.Y.Hu, Z.K.Liu and L.Q.Chen: *Acta Mater.*, Vol. 50 (2002), p.395.
[5] A.G.Khachaturyan: *Theory of Structural Transformations in Solids*, John Wiley and Sons, New York, (1983).
[6] L.Q.Chen and J.Shen: *Comput. Phys. Commun.*, Vol. 108 (1998), p.147.
[7] J.E.Breedis and C.M.Wayman: *Trans. Metall. Soc. AIME*, Vol. 224 (1962), p.1128.
[8] G.Hausch and H.Warlimont: *Acta Metall.*, Vol. 21 (1973), p.401.